Journal of Colloid and Interface Science 333 (2009) 304–309

Contents lists available at ScienceDirect

Journal of Colloid and Interface Science

www.elsevier.com/locate/jcis

Fabrication and adhesion of biomimetic nanotextures fabricated by local oxidation nanolithography

Yufei Mo [a,b], Mingwu Bai [a,*]

[a] State Key Laboratory of Solid Lubrication, Lanzhou Institute of Chemical Physics, Chinese Academy of Sciences, Lanzhou 730000, PR China
[b] Graduate School of Chinese Academy of Sciences, Beijing 100039, PR China

ARTICLE INFO

Article history:
Received 18 November 2008
Accepted 21 January 2009
Available online 24 January 2009

Keywords:
Biomimetics
Nanotexture
Local anodic oxidation
Atomic force microscopy
Adhesion

ABSTRACT

Functional surfaces with biomimetic nanotexture have aroused much interest because of their great advantages in applications. The nanometer-sized biomimetic textures are fabricated using current induced local anodic oxide (LAO) method. By controlling pulsed bias voltage, pulsewidth and relative humidity, the dimensions of biomimetic textures can be precisely controlled. In our study, an atomic force microscopy (AFM) is used for both fabrication and characterization. Conductive AFM allows fabrication process of biomimetic nanotexture without the need to change masks or repeat entire fabrication process. Furthermore, the adhesive characterization of the biomimetic nanotexture was investigated by a colloidal probe.

1. Introduction

Functional surfaces with biomimetic texture have aroused much interest because of their great advantages in applications. The geometrical structure of the surface together with chemical composition governs the properties of solid surface. Some plat leaves and bodies of animals are known to control adhesion, friction and wettability. Inspired by these living organisms in nature, artificial surfaces with some textures are commonly fabricated through many methods such as crystallization control [1], phase separation [2,3], molding [4], anodic oxidization of aluminum [5], immersion of porous alumina gel films in boiling water [6], electrochemical deposition [7,8] and chemical vapor deposition [9,10]. However, all these methods cannot produce surfaces with biomimetic textures, and also they are with high cost. In our previous study [11], we successfully duplicated original biological surface on nickel surface combining template duplication and electroplating methods. Unfortunately, this method can only well produce biomimetic texture at micrometer scale, furthermore, the duplicate sheets were no flat at macroscale due to internal stress. Over the past years, nanostructures and nanodevices have attracted tremendous attention as well as physical challenges in ultimately scaled designs for the future. The challenge in the methodology is the biomimetic patterns using in surfaces of the nanodevices.

Patterns with dimension of 100 nm or larger have been fabricated using photolithography [12,13], microcontact printing [14–18], microwriting [19,20] and micromachining [21]. Ion and electron beam lithography have produced patterns within the films with dimensions of tens of nanometers under ultra high vacuum conditions [22–24]. Scanning probe lithography (SPL), nanoparticles mask and nanografting have produced patterns with dimensions of several nanometers within self-assembled monolayers (SAMs) [25–27]. The nanopattern SAMs produced via SPL or nanografting have primarily been negative patterns or in solutions [28–30]. The challenging task remains to produce more microscopies such as nanometer or molecular-scale, patterns of controlled lateral metrology [29]. Local anodic oxidation (LAO) by the atomic force microscope (AFM) is one of the lithography technique perspectives for fabrication of nanometer-scaled structures and devices [31,32]. AFM-LAO is base on a direct oxidation of the sample by negative voltage applied to the AFM tip with respect to the surface of sample. The AFM-LAO process can be used in not only fabrication of nanodevices but also adhesion-resistance and friction-reduction as surface textures [33,34]. In previous studies, AFM-LAO has been demonstrated as the most promising tool for fabricating nanodots and lines on several types of materials ranging from metals and semiconductors [35–43].

AFM has been used extensively to measure adhesive forces between the contact surfaces in nanoscale. Adhesive forces come from two sources: contact interfacial forces and non-contact forces such as Van Der Waals or electrostatic forces. Adhesion is typically measured by pull-off force between the cantilever tip and the surface. The challenge in the measurement often lies with the determination of real area of contact. For sharp tip, the surface roughness and high contact pressure may cause the tip to rotate and the surface to deform. Ducker [44] introduced the use

* Corresponding author. Fax: +86 931 4968163.
E-mail address: mwbai@lzb.ac.cn (M. Bai).

0021-9797/$ – see front matter
doi:10.1016/j.jcis.2009.01.039

Table 1
List of the biological originals examined in this study.

Species	Locality	Habitat
Rice leaf	Hanzhong city, Shanxi province	Paddy field, hydrophily
Dung beetle	Lanzhou city, Gansu province	Insect

of colloidal probe tips by attaching a sphere to the cantilever to measure adhesion. The spherical shape of the tip provides controlled contact pressure, symmetry, and mostly elastic contacts. To LAO nanotexture adhesion measurement, the spherical probe tip can fully contact with texture surface, while sharp tip can only point contact. However, the measurement of the contact surface roughness of a colloidal probe poses additional challenges, since the total surface area are very small. Therefore, we adopted the reverse AFM imaging method developed by Neto [45] to identify the contact location and direct imaged by an AFM with a sharp tip to provide detailed three-dimensional surface topography.

In this paper, we introduce a new method for biomimetic nanotexture using current induced LAO. In our approach, the topographic images of living creature surfaces were first imaged using scanning electron microscope (SEM). The data of image were then translated to a script program for the well-defined movement of the tip over a sample. The LAO process is well controlled by several major parameters as follows: pulsed bias voltage, pulsewidth and humidity. The desired dimension of pre-designed nanotexture can be fabricated by controlling these parameters. The nanostructures replicated from the biological originals suggest that this technique can achieve features with resolution as high as nanometer-sized on Si surface. Furthermore, the adhesive characterization of the biomimetic nanotextures was investigated by a colloidal probe.

2. Experimental

Biological originals (rice leaf, dung beetle), the localities of which and their corresponding habitats are shown in Table 1.

The H-passivated Si (P-type 100) wafers, obtained from Benyuan Technology Co. Ltd., Beijing, were used as substrate. The wafers were ultrasonicated in acetone followed by isopropanol for 5 min each before use. The H-passivated Si substrate is hydrogen passivated by leaking H_2 into an ultrahigh vacuum (UHV) chamber, where atomic H was created by creaking H_2 molecules on a hot tungsten filament. The process can prevent silicon converting to a nonuniform native oxide. In order to improve resolution of oxide nanotextures and investigate their adhesive properties, we focus on fabrication of biomimetic nanotextures on H-passivated Si substrate by LAO.

The morphologies of these samples of living creature surfaces and their replicates were observed on a JSM-5600LV scanning electron microscope (SEM).

Fabrication of biomimetic nanotexture was performed by using a commercial AFM (CSPM 4000). The LAO was carried out in contact mode and in the regime of the contact force using silicon cantilevers with electrically conductive tips coated by platinum (Budget sensor). The tip is conic and the radius is below 25 nm. The AFM software was extended with a program package for the well-defined movement of the tip over a sample. The facility associated with control of other tip-sample parameters gave us possibility to accomplish pre-defined patterns at various pulsed bias voltage, pulsewidth and write speed in contact mode. For environmental control, relative humidity was controlled by introducing a mixture of dry and moist nitrogen stream inside the booth, while the temperature was maintained at $10 \pm 1\,^{\circ}C$. The relative humidity was controlled to range from 15 to 80%. In this nanolithography process, oxides grow on a chemically reactive substrate by the application of a pulse bias voltage between a conductive tip and a sample surface which acts as an anode. The LAO process performed by AFM is illustrated in Fig. 1. The driving force is the faradaic current flows between the tip and sample surface with the aid of the water meniscus. When the faradaic current flows into water bridge, H_2O molecules are decomposed into oxyanions (OH^-, O^-) and protons (H^+). These ions penetrate into the oxide layer due to a high electric field ($E > 10^7$ V/m) [46], leading to the formation and subsequent growth of SiO_2 on the Si surface.

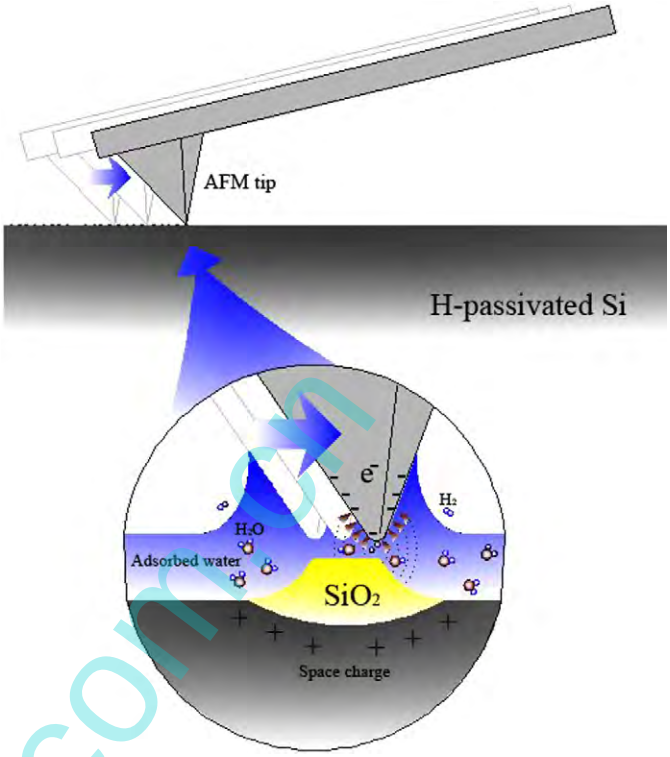

Fig. 1. Schematic drawing of the local anodic-oxidation process induced by a biased conductive AFM tip.

For adhesion measurement of the fabricated nanotextures, colloidal probe was prepared by gluing glass sphere with a radius of 40 μm onto individual tipless cantilever. The cantilever used in our experiments was etched from single-crystal silicon, and the force constant of the cantilever was calculated using the individually measured thickness, width and length [47]. The above dimensions were determined by a scanning electron microscope, and the normal force constant of the cantilever was determined to be 0.275 N/m, which is close to the announced force constant 0.30 N/m. A typical colloidal probe is shown in Fig. 2. The colloidal probe was cleaned by ethanol and acetone in turn before use. For all measurements the same cantilever was used in this comparative study. Furthermore, to avoid influence of molecules which may transfer to the tip on the AFM/FFM experiments, the tip was scanned on a cleaved mica surface to remove these physical adsorbed molecules. The surface topography of the colloidal probe was scanned with a force constant of 0.12 N/m cantilever and a silicon nitride sharp tip under contact mode, as shown in Fig. 3. The relative humidity was controlled at 15% RH. Repeated measurements were within 5% of the average value for each sample.

3. Results and discussion

Dung beetle surface and rice leaves show hydrophobic and low adhesion, which is due to the presence of microbump on surfaces

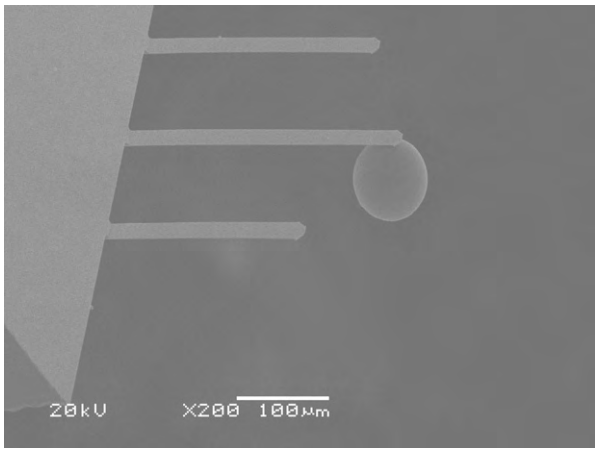

Fig. 2. SEM image of the colloidal probe.

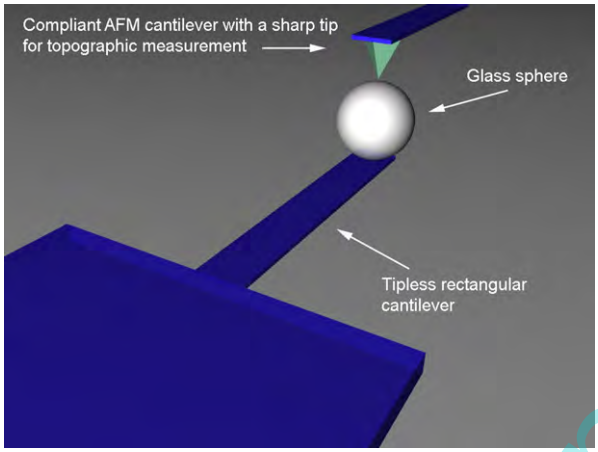

Fig. 3. A schematic illustration on topographic measurement of colloidal probe.

of the leaves [48–50]. Fig. 4a shows the SEM image of the surface of dung beetle. On the surface, the papillae with the average diameter about 40–60 μm are arranged and the distance between the adjacent papillae is about 60–100 μm in this dimension. Figs. 4b and 4c present the AFM topographic and corresponding lateral force images of its miniature replica. On the replica surface, the diameter of the papillae is about 1.5–3 μm and the distance between the adjacent papillae is about 2–4 μm. The height of original was examined with a profiler. The cursor profile shown in Fig. 5 reveals that the height of the papillae is about 24–27 μm. The 3D AFM image and the corresponding cursor profile of the miniature replica are shown in Figs. 6a and 6b, respectively. From the figure, the papillae with the average height about 1–2 nm are arranged on the silicon surface.

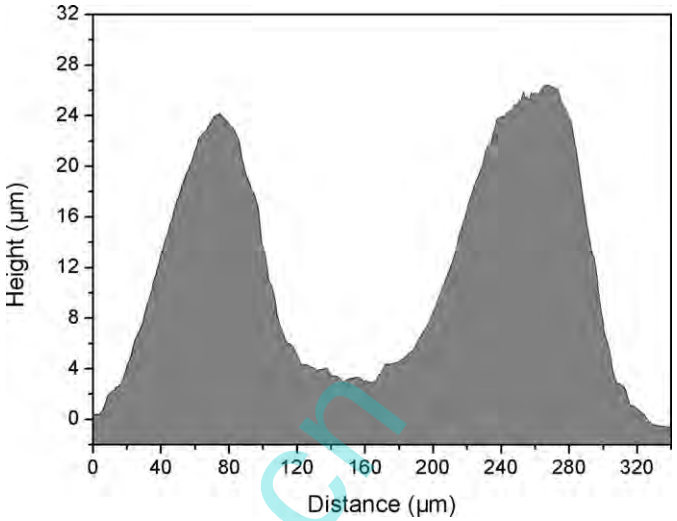

Fig. 5. The cursor profile of surface of biological original of dung beetle.

Fig. 7 shows SEM image the surface of rice leaf and AFM image of its replica. Fig. 7a indicates a one-dimensional ordered structure on the surface of rice leaf, on which there is papillae. On the original surface, the papillae with average diameter about 2–5 μm are arranged and the distance between the adjacent papillae is about 5–10 μm in this dimension. The height of papillae is about 2–4 μm. Figs. 7b and 7c show the AFM topographic and corresponding lateral force images of its miniature replica. On the replica surface, the diameter of the papillae is about 0.4–1.5 μm and the distance between the adjacent papillae is about 0.5–2 μm. The 3D AFM image and the corresponding cursor profile of the miniature replica are shown in Figs. 8a and 8b, respectively. From the figure, the papillae of rice leaf with the average height about 2.5–4 nm are arranged on the silicon surface.

Fig. 9 shows the oxide height of the biomimetic nanotexture as a function of relative humidity for various plus bias voltage and pulsewidth. It is evident that the lower pulse bias voltages and short pulsewidths result in lower oxide texture. The reason for that could be due to no enough voltage or time for reaching the saturation height. In anodic-oxidation process, the anionic and cationic transports are important factors in determining the kinetics of oxidation. In this figure, the height of Si oxide nanotexture was proportional to relative humidity for two distinct pulse bias voltage and pulsewidth. The reason for that could be due to the differences in the thickness of the water film.

Adhesion is generally measured by the amount of force necessary to separate two surfaces in contact. In nanoscale, mechanical loading is often not the overwhelming force as in macroscale, and surface forces such as Van Der Waals, electronic, and capillary/meniscus forces become significant in controlling the pull-off

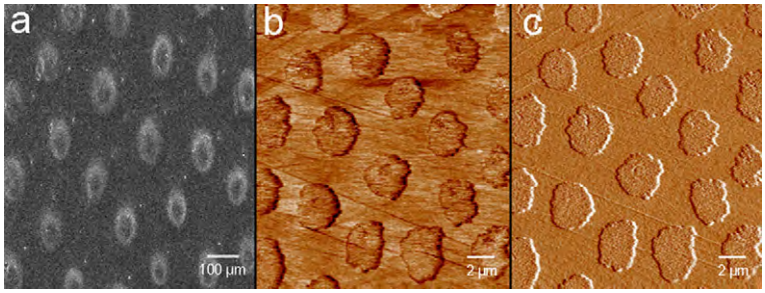

Fig. 4. The SEM image (a) of the surface of dung beetle and AFM image of its replica. (b) Topographic scan of the replica. (c) Corresponding of frictional force image of (b).

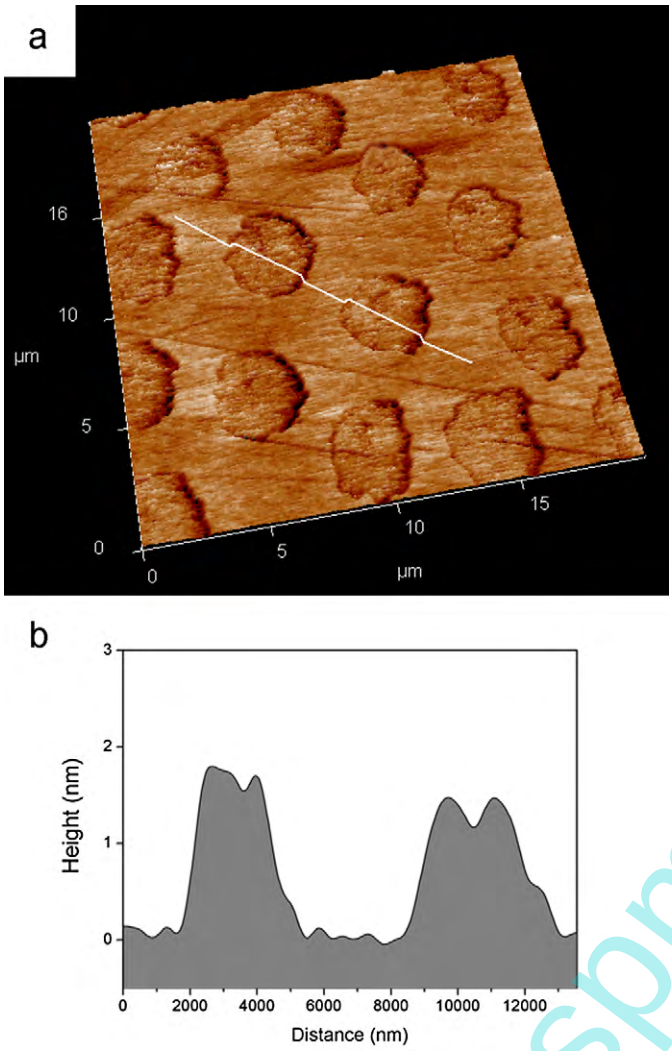

Fig. 6. The 3D AFM image (a) and corresponding cursor profile (b) of the miniature replica of dung beetle.

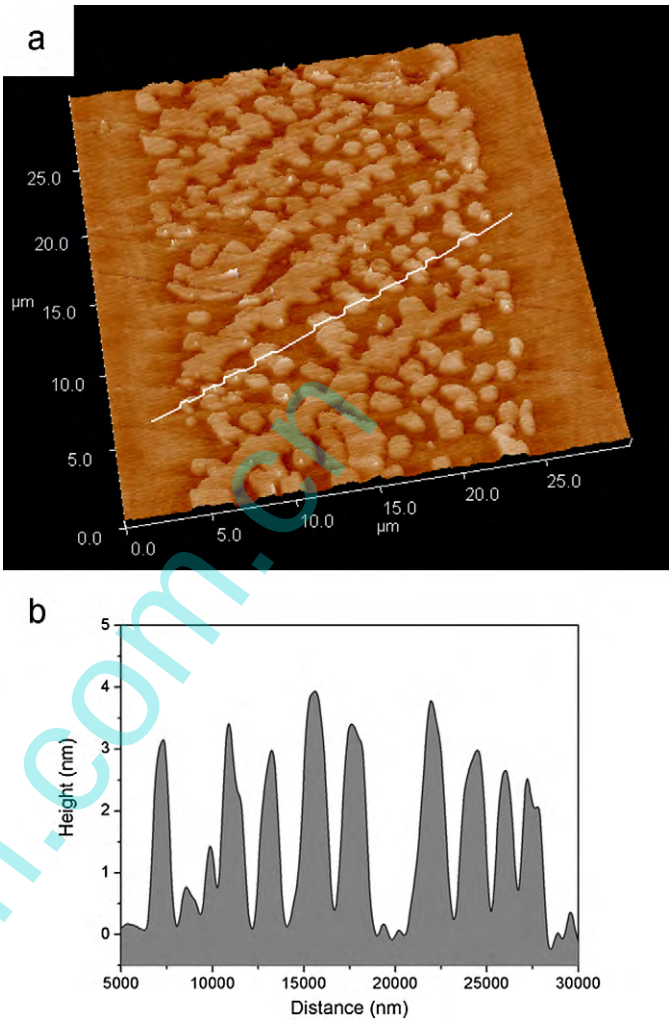

Fig. 8. The 3D AFM image (a) and corresponding cursor profile (b) of the miniature replica.

force. Fig. 10 shows the three-dimensional surface topography of a colloidal probe. The microroughness of the colloidal probe in root-mean-square (RMS) of the monolayer was estimated to be 0.1 nm over an area of 1 um × 1 um (512 × 512 resolution). The adhesive force between the colloidal probe and sample surfaces are shown in Fig. 11. Strong adhesive force was observed on the untreated H-passivated silicon surface, on which the adhesive force was about 175 nN. After the biomimetic nanotextures of rice leaf and dung beetle were generated, the adhesive force was decreased to 87 and 96 nN, respectively. This indicates that the biomimetic nanotexture exhibited adhesion resistance.

4. Summary and conclusions

In the paper, the application of current induced LAO for the fabrication of biomimetic nanotextures is presented. In our ap-

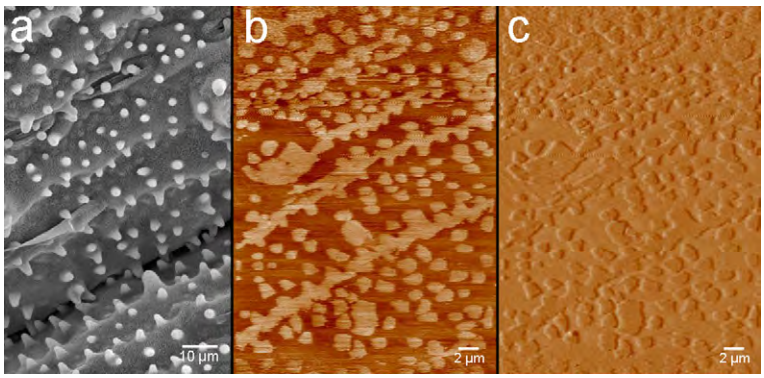

Fig. 7. The SEM image (a) of the surface of rice leaf and AFM image of its replica. (b) Topographic scan of the replica. (c) Corresponding of frictional force image of (b).

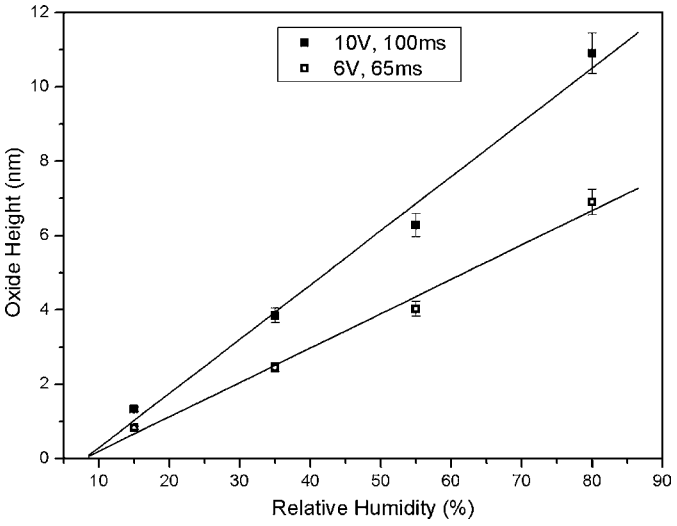

Fig. 9. The height of Si oxide as a function of relative humidity for two distinct optional parameters (pulse bias voltage and pulsewidth).

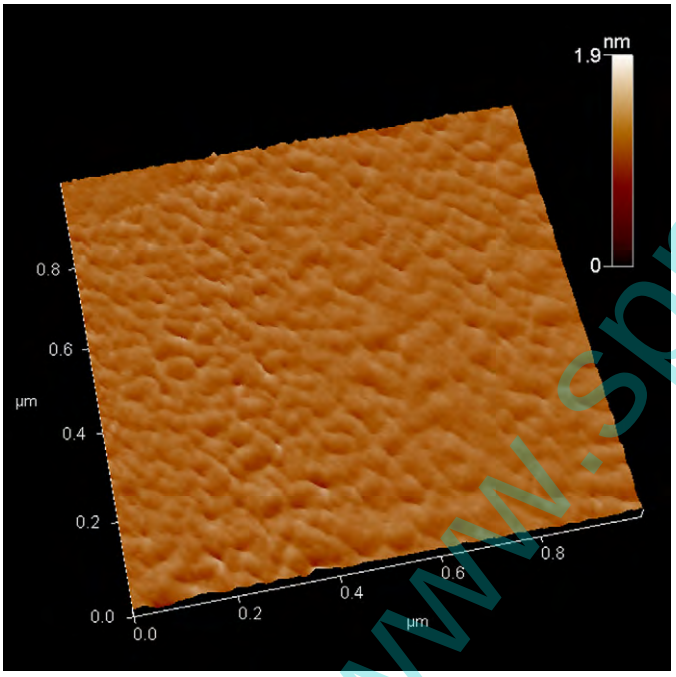

Fig. 10. AFM topographic scan of the spherical tip of colloidal probe.

proach, the surfaces of dung beetle and rice leaf were proportionate miniature replicated on H-passivated Si surface. The experimental results show that the AFM current induced LAO can be a viable tool for fabricating spatially well-defined and controlled biomimetic nanotexture provided proper operation conditions are chosen. The lowest value of the height of the biomimetic nanotexture was about 1 nm. The H-passivated Si treated with biomimetic nanotextures exhibit better adhesive resistance than untreated Si in nanoscale. It is expected that this approach could be extended to duplicate other biological and artificial template surface on silicon surface. These surfaces with special nanotextures are great importance for both fundamental research and practical applications such as microhydromechanics, wettability, biosensors and biochips.

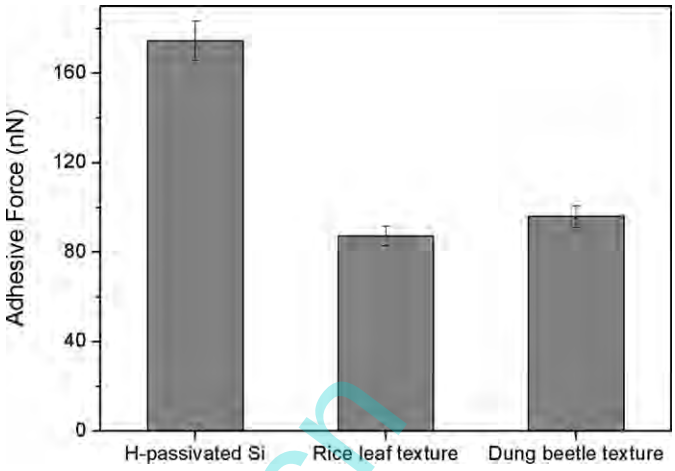

Fig. 11. Adhesive forces between AFM colloidal probe and surfaces of bare H-passivated Si, rice leaf texture and dung beetle texture.

Acknowledgment

This work was funded by National Natural Science Foundation of China (NSFC) under Grant Number 20773148, and National 973 Program: 2007CB607601.

References

[1] S. Shibuichi, T. Onda, N. Satoh, K. Tsujii, Langmuir 12 (1996) 2125.
[2] J.T. Han, X.R. Xu, K.W. Cho, Langmuir 21 (2005) 6662.
[3] N.J. Shirtcliffe, G. McHale, M.I. Newton, C.C. Perry, Langmuir 19 (2003) 5626.
[4] J. Bico, C. Marzolin, D. Quéré, Europhys. Lett. 47 (1999) 220.
[5] K. Tsujii, T. Yamamoto, T. Onda, S. Shibuchi, Angew. Chem. Int. Ed. Engl. 36 (1997) 1011.
[6] K. Tadanaga, N. Katata, T. Minami, J. Am. Ceram. Soc. 80 (1997) 3213.
[7] X. Zhang, F. Shi, X. Yu, H. Liu, Y. Fu, Z. Wang, L. Jiang, X. Li, J. Am. Chem. Soc. 126 (2004) 3064.
[8] N.J. Shirtcliffe, G. McHale, M.I. Newton, G. Chabrol, C.C. Perry, Adv. Mater. 16 (2004) 1929.
[9] Y. Wu, H. Sugimura, Y. Inoue, O. Takai, Chem. Vap. Deposition 8 (2002) 47.
[10] K.K.S. Lau, J. Bico, K.B.K. Teo, M. Chhowalla, G.A.J. Amaratung, W.I. Milne, G.H. McKinley, K.K. Gleason, Nano Lett. 3 (2003) 1701.
[11] Y. Wang, Y. Mo, M. Zhu, M. Bai, Surf. Coat. Technol. 203 (2008) 137.
[12] Y.Y. Huang, D.A. Dahlgren, J.C. Hernminger, Langmuir 10 (1994) 626.
[13] M.J. Tarlov, D.R.F. Burgess, G. Gillen, J. Am. Chem. Soc. 115 (1993) 5305.
[14] G.P. Lopez, M.W. Albers, S.L. Schreiber, R. Carroll, E. Peralta, G.M. Whitesides, J. Am. Chem. Soc. 115 (1993) 5877.
[15] N.L. Jeon, R.G. Nuzzo, Y. Xia, M. Mrksich, G.M. Whitesides, Langmuir 11 (1995) 3024.
[16] N. Jeon, W. Lin, M.K. Frhardt, G.S. Girolami, R.G. Nuzzo, Langmuir 13 (1997) 3833.
[17] Y. Xia, G.M. Whitesides, Angew. Chem. Int. Ed. Engl. 37 (1998) 550.
[18] M. Husemann, D. Mecerreyes, C.J. Hawker, J.L. Hedrick, R. Shah, N.L. Abbott, Angew. Chem. Ed. Engl. 38 (1999) 647.
[19] A. Kumer, M.A. Biebuyck, N.L. Abbott, G.M. Whitesides, J. Am. Chem. Soc. 114 (1992) 9188.
[20] N.L. Abbott, A. Kumar, G.M. Whitesides, Chem. Mater. 6 (1994) 596.
[21] N.L. Abbott, J.P. Folkers, G.M. Whitesides, Science 257 (1992) 1380.
[22] D.L. Allara, R.C. Tiberio, H.G. Craighead, M. Lercel, Appl. Phys. Lett. 62 (1993) 476.
[23] K.K. Berggren, A. Bard, J.L. Wilbur, J.D. Gillaspy, A.G. Helg, J.J. McClelland, S.L. Rolston, W.D. Phillips, M. Prentiss, G.M. Whitesides, Science 269 (1995) 1255.
[24] J.A.M. Sondag-Huethorset, H.R.J. Van Helleputte, L.G.J. Fokkink, Appl. Phys. Lett. 64 (1994) 285.
[25] C.B. Ross, L. Sun, R.M. Crook, Langmuir 9 (1993) 632.
[26] R.D. Piner, J. Zhu, F. Xu, S.H. Hong, C.A. Mirkin, Science 283 (1999) 661.
[27] Y.F. Mo, M.W. Bai, J. Phys. Chem. C 112 (2008) 11257.
[28] D. Xiao, G.Y. Liu, D.H. Charych, M. Salmeron, Langmuir 11 (1995) 1600.
[29] S. Xu, S. Miller, P.E. Laibinis, G.Y. Liu, Langmuir 15 (1999) 7244.
[30] K. Wadu-Mesthrige, S. Xu, N.A. Amro, G.Y. Liu, Langmuir 15 (1999) 8580.
[31] J.A. Dagata, Science 270 (1995) 1625.
[32] R. Garcia, R.V. Martinez, J. Martinez, Chem. Soc. Rev. 35 (2006) 29.
[33] Y.F. Mo, Y. Wang, M.W. Bai, Physica E 41 (2008) 146.
[34] Y.F. Mo, Y. Wang, J.B. Pu, M.W. Bai, Langmuir 25 (2009) 40.

[35] Z. Chen, S. Hou, H. Sun, X. Zhao, J. Phys. D Appl. Phys. 37 (2004) 1357.
[36] P. Avouris, T. Hertel, R. Martel, Appl. Phys. Lett. 71 (1997) 285.
[37] M. Yang, Z. Zheng, Y. Liu, B. Zhang, Nanotechnology 17 (2006) 330.
[38] Y. Okada, S. Amano, M. Kawabe, J.S. Harris, J. Appl. Phys. 83 (1998) 7998.
[39] S.R. Jian, T.H. Feng, D.S. Chuu, J. Phys. 38 (2005) 2432.
[40] F.S. Chien, J.W. Chang, S.W. Lin, Y.C. Chou, T.T. Chen, S. Gwo, T.S. Chao, W.F. Hsieh, Appl. Phys. Lett. 76 (2000) 360.
[41] X.N. Xie, H.J. Chung, H. Xu, C.H. Sow, A.T. Wee, Appl. Phys. Lett. 84 (2004) 4914.
[42] X.N. Xie, H.J. Chung, H. Xu, C.H. Sow, A.T. Wee, J. Am. Chem. Soc. 126 (2004) 7665.
[43] S.F. Lyuksyutov, R.A. Vaia, P.B. Paramonov, S. Juhl, L. Waterhouse, R.M. Ralich, G. Sigalov, E. Sancaktar, Nat. Mater. 2 (2003) 468.
[44] W.A. Ducker, T.J. Senden, R.M. Pashley, Nature 353 (1991) 239.
[45] C. Neto, v.S.J. Craig, Langmuir 17 (2001) 2097.
[46] S.R. Jian, T.H. Fang, D.S. Chuu, J. Phys. D Appl. Phys. 38 (2005) 2432.
[47] Y.H. Liu, T. Wu, D.F. Evans, Langmuir 10 (1994) 2241.
[48] T.L. Sun, L. Feng, X.F. Gao, L. Jiang, Acc. Chem. Res. 38 (2005) 644.
[49] L. Feng, Y.L. Song, J. Zhai, B.Q. Liu, J. Xu, L.D. Jiang, B. Zhu, Angew. Chem. Int. Ed. 42 (2003) 800.
[50] Z. Burton, B. Bhushan, Ultramicroscopy 106 (2006) 709.